RAA 2017 Vol. **17** No. **12**, 123 (12pp) doi: 10.1088/1674–4527/17/12/123

http://www.raa-journal.org *http://iopscience.iop.org/raa*

Research in Astronomy and Astrophysics

Dependence of large SEP events with different energies on the associated flares and CMEs

Gui-Ming Le[1,2] and Xue-Feng Zhang[2]

[1] Key Laboratory of Space Weather, National Center for Space Weather, China Meteorological Administration, Beijing 100081, China; *legm@cma.gov.cn*

[2] School of Computer Science, Anhui University of Technology, Maanshan 243032, China

Received 2017 July 10; accepted 2017 August 24

Abstract To investigate the dependence of large gradual solar energetic particle (SEP) events on the associated flares and coronal mass ejections (CMEs), the correlation coefficients (CCs) between peak intensities of $E > 10\,\mathrm{MeV}$ (I_{10}), $E > 30\,\mathrm{MeV}$ (I_{30}) and $E > 50\,\mathrm{MeV}$ (I_{50}) protons and soft X-ray (SXR) emission of associated flares and the speeds of associated CMEs in the three longitudinal areas W0–W39, W40–W70 (hereafter the well connected region) and W71–W90 have been calculated. Classical correlation analysis shows that CCs between SXR emission and peak intensities of SEP events always reach their largest value in the well connected region and then decline dramatically in the longitudinal area outside the well connected region, suggesting that they may contribute to the production of SEPs in large SEP events. Both classical and partial correlation analyses show that SXR fluence is a better parameter describing the relationship between flares and SEP events. For large SEP events with source location in the well connected region, the CCs between SXR fluence and I_{10}, I_{30} and I_{50} are 0.58±0.12, 0.80±0.06 and 0.83±0.06 respectively, while the CCs between CME speed and I_{10}, I_{30} and I_{50} are 0.56±0.12, 0.52±0.13 and 0.48±0.13 respectively. The partial correlation analyses show that in the well connected region, both CME shock and SXR fluence can significantly affect I_{10}, but SXR peak flux makes no additional contribution. For $E > 30\,\mathrm{MeV}$ protons with source location in the well connected region, only SXR fluence can significantly affect I_{30}, and the CME shock makes a small contribution to I_{30}, but SXR peak flux makes no additional contribution. For $E > 50$ MeV protons with source location in the well connected region, only SXR fluence can significantly affect I_{50}, but both CME shock and SXR peak flux make no additional contribution. We conclude that these findings provide statistical evidence that for SEP events with source locations in the well connected region, a CME shock is only an effective accelerator for $E < 30\,\mathrm{MeV}$ protons. However, flares are not only effective accelerators for $E < 30\,\mathrm{MeV}$ protons, but also for $E > 30\,\mathrm{MeV}$ protons, and $E > 30\,\mathrm{MeV}$ protons may be mainly accelerated by concurrent flares.

Key words: Sun: coronal mass ejections (CMEs) — Sun: flares — (Sun:) particle emission

1 INTRODUCTION

There are two kinds of solar energetic particle (SEP) events, named impulsive and gradual SEP events respectively. The former is accompanied by an impulsive flare, while the latter is accompanied by both a gradual flare and a fast coronal mass ejection (CME), and the intensity-time profile of solar proton events (SPEs) can be used to predict the geoeffectiveness of the CMEs associated with SPEs (Le et al. 2016). Nobody doubts that the solar source of an impulsive SEP event is associated with an impulsive flare. However, when a gradual SEP event happens, whether the concurrent flare contributes to the SEP event is still an open question. There are two points of view on the solar source of gradual SEP events. The first one is that only CME-driven shocks contribute to gradual SEP events (e.g. Reames 1999; Tylka et al. 2005). The second one is that the solar source of a gradual SEP event may be both concurrent flare and shock driven by the associated CME (e.g., Kallenrode 2003; Trottet et al. 2015). Cane et al. (2007) suggested that solar flares and CMEs are likely to coexist and the evolution of any event depends on the relative importance of the processes. This is also consistent with the statement (Firoz et al. 2012) that type III and type II bursts are successive evolutions and it is difficult to separate them. Andriopoulou et al. (2011) suggested that it difficult to determine which the dominant acceleration mechanism is in each ground level enhancement (GLE) case. Investigation of the properties of SEPs inferred from their associated radio emission suggests that a clear-cut distinction between flare-related and CME-related SEP events is difficult to establish (Kouloumvakos et al. 2015). Some cases and statistical studies (e.g. Miroshnichenko et al. 2005; Aurass et al. 2006; Le et al. 2006; Simnett 2006; Li et al. 2007a,b, 2009; Bazilevskaya 2009; Masson et al. 2009; Grechnev et al. 2008; Pérez-Peraza et al. 2009; Aschwanden 2012; Le et al. 2013; Klein et al. 2014) have shown that relativistic solar protons (RSPs) may be accelerated by concurrent flares. Some statistical investigations have also been devoted to studying the relationship between peak intensities of SEP events and parameters of the associated solar flares and CMEs (e.g. Dierckxsens et al. 2015; Grechnev et al. 2015; Trottet et al. 2015). However, longitudinal dependence of peak intensities of SEP events on associated flares has not been investigated in the literature (Dierckxsens et al. 2015; Grechnev et al. 2015; Trottet et al. 2015). The longitudinal dependence of peak intensities of SPEs on soft X-ray (SXR) peak flux has been investigated by Park et al. (2010). However, the longitudinal area was divided into E90–E30, E30–W30 and W30–W90 and only the correlation coefficients (CCs) between peak intensities of SPEs and flare intensities in these three longitudinal areas have been calculated. It is evident that Park et al. (2010) did not calculate the CC between SXR peak flux and peak intensities of SPEs in the well connected region (W40–W70), and the relationship between SXR fluence and peak intensities of SPEs was not investigated in their paper.

It has been accepted that SEPs accelerated by a CME-driven shock can be observed in a very large longitudinal area, but flare-accelerated particles can only be observed in a small longitudinal area, especially in the longitudinal area well connected with the source location of an associated SEP event. When a solar flare is an eruptive flare, the accompanying CME will open the magnetic field over the associated active region (AR), leading to the flare-accelerated particles escaping from the AR and then entering interplanetary space. Because the magnetic field lines over an AR are very complicated and SEPs can not only propagate along the magnetic field lines, but can also propagate along the direction perpendicular to the magnetic field lines (Bieber et al. 2004; Qin 2007; Qin et al. 2013; Qin & Zhang 2014; Qin & Wang 2015), flare-accelerated particles can not only can be observed in the longitudinal area well connected with the SEP source region, but also can be observed in the longitudinal area outside the well connected region. However, the largest flux of flare-accelerated particles can only be observed in the longitudinal area well connected with the SEP source location. When a large gradual SEP event happens, if a lot of satellites can be used to observe the SEP flux at every magnetic field line, then it is easy to check whether the SEP flux is longitudinally dependent and reaches its largest flux in the longitudinal area well connected with the SEP source location, which can be used to judge whether associated flares contribute to the production of SEPs in a large gradual SEP event. However, there has not been this kind of SEP data. Statistical correlation analysis can also be used to judge whether flares contribute to the production of SEPs. If flares really contribute to the production of SEPs in large gradual SEP events, then flares should have a good correlation with the peak intensities of SEP events in the well connected region, but flares should have poor correlation with the peak intensities of SEP events in the longitudinal area outside the well connected region. Classical and partial correlation analyses for the relationship between the peak intensities of $E \geq 100$ MeV protons and parameters of associated flares and CMEs in the well connected region and in the longitudinal area outside the well connected region have been investigated. The results suggest that, for SEP events with source location in the well connected region, $E \geq 100$ MeV protons may be mainly accelerated by concurrent flares (Le et al. 2017).

In this paper, the relationship between the parameters of flares and CMEs and the peak intensities of protons with different energies lower than 100 MeV in the well connected region and in the longitudinal area outside the well connected region will be investigated.

This is the motivation of the paper. Data sources and definitions are presented in Section 2. The associated classical correlation analysis is presented in Section 3. Section 4 describes the related partial correlation analysis. Section 5 is the summary and discussion, and conclusions are presented in the final section.

2 DATA SOURCES AND DEFINITIONS

A large gradual SEP event, or an SPE, is defined as the proton peak flux ≥ 10 pfu (particle flux unit, particle cm^{-2} sr^{-1} s^{-1}) in the $E > 10$ MeV channel as measured by the *Geostationary Operational Environmental Satellite* (*GOES*) spacecraft during an SEP event accompanied by both a fast CME and a long duration SXR flare. When a large gradual SEP event happens, the flux of protons with different energies, such as $E > 10$, $E > 30$ and $E > 50$ MeV protons and even higher energy protons may increase at almost the same time, however, the peak fluxes of protons with different energies are different.

The time integral of SXR flux for a flare, fluence (Φ_x), is defined as

$$\Phi_x = \int_{t_\mathrm{s}}^{t_\mathrm{e}} \Big[f(t) - f(t_\mathrm{s})\Big] dt, \qquad (1)$$

where $f(t)$ is the SXR flux, and t_s and t_e are the start and end times of the SXR flare, respectively. Equation (1) indicates that SXR flux, from which the background has been subtracted, is integrated over the flare start to end times. The flare start, peak and end times have been defined by SEC/NOAA. The flare end time was defined as the time when SXR flux decayed to a middle point between SXR peak flux and background SXR flux (Kubo & Akioka 2004). Φ_x is related to the total energy released by the associated flare (Kubo & Akioka 2004; Chen et al. 2016), indicating that Φ_x is a better parameter for describing the properties of SXR emission than SXR peak flux, and SXR fluence has a better correlation with peak flux of 15–40 MeV protons than SXR peak flux (Trottet et al. 2015).

The SXR flare start, peak and end times, and the SXR fluence, are obtained from (*ftp://ftp.ngdc.noaa.gov /STP/space-weather/solar-data/*). The peak intensity of $E > 10$, $E > 30$ and $E > 50$ MeV protons observed by *GOES* during solar cycle 23 were obtained from the website (*http://spidr.ngdc.noaa.gov/spidr/*). It can be noticed that the proton data observed by *GOES* have been removed from the website (*http://spidr.ngdc.noaa.gov/spidr/*). For SPEs that occurred during solar cycle 23, the source location, CME speed and flare intensity for each SPE can be directly copied from the paper Cane et al. (2010). The CME speed associated with SPE that occurred on 2005 January 20 used in the paper is 3242 km s^{-1} (Gopalswamy et al. 2005). The SPEs that occurred during solar cycle 24 are available from (*http://umbra.nascom.nasa.gov/sdb/goes/particle/*).
The linear speed of a CME, V_CME, can be obtained from the CME catalog (Yashiro et al. 2004, *http://cdaw.gsfc.nasa.gov/CME_list/*) of *Solar and Heliospheric Observatory*/Large Angle Spectroscopic Coronagraph (*SOHO*/LASCO; Brueckner et al. 1995).

The source location that is magnetically well connected with the Earth should be located in the west hemisphere of the Sun. Seventy-nine SPEs with source locations in the west hemisphere that occurred during 1997–2014 were selected and are listed in Table 1.

In the table, SPEs are numbered in Col. (1), the year and date of the events in Cols. (2) and (3) respectively, the time when SXR flux reached its peak value in Col. (4), the location of the flare site in Col. (5), SXR peak flux, I_SXR, in Col. (6), SXR fluence in Col. (7), the linear speed of the CME in Col. (8), the peak intensity of $E > 10$ MeV protons, I_{10}, in Col. (9), the peak intensity of $E > 30$ MeV protons, I_{30}, in Col. (10), and the peak intensity of $E > 50$ MeV protons, I_{50}, in Col. (11). The CME speed associated with the SPE that occurred on 2005 January 20 estimated by Gopalswamy et al. (2005) is 3242 km s^{-1}, which will be used in the paper.

3 CLASSICAL CORRELATION ANALYSIS AND RESULTS

Because our sample only comprises 79 SPEs, we also use the bootstrap method (Wall & Jenkins 2012) to estimate the statistical uncertainty of CCs, which was used by Trottet et al. (2015). The CCs were calculated for N pairs of values chosen at random within the set of N observations. This procedure was repeated 5000 times.

3.1 Correlation between SEPs and SXR Peak Flux

The source locations well connected with the Earth are mainly distributed in the longitudinal area ranging from W40 to W70, which can be seen from figure 2.3 in the paper Reames (1999). The CCs between peak intensities of SEP events and SXR peak flux in three longitudinal areas: W0–W39, W40–W70 and W71–W90 have been

Table 1 The Parameters of Flares and CMEs Associated with Large Gradual SEP Events during 1997–2014

No.	Year yyyy	Date mm/dd	Time hh:mm	Location	$I_{\rm SXR}$ (SXR peak flux)	$\Phi_{\rm SXR}/10^3$ (erg cm^{-2})	$V_{\rm CME}$ (km s^{-1})	I_{10} (pfu)	I_{30} (pfu)	I_{50} (pfu)
(1)	(2)	(3)	(4)	(5)	(6)	(7)	(8)	(9)	(10)	(11)
1	1997	11/04	05:55	S14W33	X2.1	5.60E–02	785	72	20.3	9.98
2	1997	11/06	11:50	S18W63	X9.4	3.60E–01	1556	490	189	115
3	1998	04/20	10:00	S43W90	M1.4	6.10E–02	1863	1700	384	103
4	1998	05/02	13:35	S15W15	X1.1	6.70E–02	938	150	48	24.3
5	1998	05/06	08:00	S11W65	X2.7	2.10E–01	1099	210	47.5	19.3
6	1998	11/05	19:00	N26W18	M8.4	1.10E–01	1118	11	0.94	0.328
7	1999	06/04	07:03	N17W69	M3.9	2.40E–02	2230	64	3.7	0.93
8	2000	04/04	15:41	N16W66	C9.7	2.30E–02	1188	55	0.99	0.321
9	2000	06/10	17:02	N22W38	M5.2	7.30E–02	1230	46	4.22	1.57
10	2000	07/14	10:24	N22W07	X5.7	7.50E–01	1674	24000	5680	1670
11	2000	07/22	11:34	N34W56	M3.7	7.00E–02	1230	17	4.22	1.57
12	2000	09/12	12:17	S17W09	M1.0	4.50E–02	1550	320	9.91	1.95
13	2000	11/08	23:28	N10W75	M7.4	2.10E–01	1738	14800	4440	1880
14	2000	11/24	14:55	N22W07	X2.3	1.60E–01	1245	100	14.7	4.98
15	2001	01/28	16:00	S04W59	M1.5	3.00E–02	916	49	6.03	1.89
16	2001	03/29	10:15	N14W12	X1.7	2.20E–01	942	35	3.93	1.15
17	2001	04/02	21:51	N18W82	X20	1.50E+00	2505	110	217	53.5
18	2001	04/10	05:26	S23W09	X2.3	3.00E–01	2411	355	14.4	3.69
19	2001	04/12	10:28	S19W42	X2.0	3.00E–01	1184	50	13.9	5.75
20	2001	04/15	13:50	S20W85	14.4	6.10E–01	1199	951	357	275
21	2001	04/26	13:12	N17W31	M7.8	9.20E–02	1006	57	0.5	0.298
22	2001	09/15	11:28	S21W49	M1.5	3.70E–02	478	11	1.26	0.45
23	2001	10/19	16:30	N15W29	X1.6	1.6E–01	901	11	2.59	1.03
24	2001	11/04	16:20	N06W18	X1.0	2.20E–01	1810	31700	1070	266
25	2001	11/22	22:30	S15W34	M9.9	3.10E–01	1437	18900	857	162
26	2001	12/26	05:40	N08W54	M7.1	3.40E–01	1446	779	331	180
27	2002	01/14	06:27	S28W83	M4.4	3.40E–01	1492	15	1.69	0.53
28	2002	02/20	06:12	N12W72	M5.1	2.20E–02	952	13	1.51	0.5
29	2002	03/15	23:10	S08W03	M2.2	1.30E–01	957	13	0.61	0.215
30	2002	03/18	02:31	S09W46	M1.0	4.50E–02	989	53	2.48	0.579
31	2002	03/22	11:14	S09W90	M1.6	4.90E–02	1750	16	0.45	0.162
32	2002	04/17	8:24	S14W34	M2.6	1.50E–01	1240	24	1.51	0.367
33	2002	04/21	01:51	S14W84	X1.5	6.00E–01	2393	2520	649	208
34	2002	05/22	03:54	S19W56	C5.0	2.50E–02	1557	820	10.2	1.15
35	2002	07/15	20:08	N19W01	M1.8	4.30E–02	1300	234	4.27	0.92
36	2002	08/14	02:12	N09W54	M2.3	6.00E–02	1309	26	0.77	0.36
37	2002	08/22	01:57	S07W62	M5.4	3.30E–02	998	36	12.6	5.98
38	2002	08/24	01:12	S08W81	X3.1	4.60E–01	1913	317	123	76.2
39	2002	11/9	13:23	S12W29	M4.6	4.80E–02	1838	404	12	1.46
40	2003	05/28	00:27	S07W17	X3.6	2.80E–01	1366	121	4.84	3.72
41	2003	05/31	02:24	S07W65	M9.3	8.50E–02	1835	27	6.79	2.92
42	2003	10/26	18:19	N02W38	X1.2	5.10E–01	1537	466	42.6	10.4
43	2003	10/29	20:49	S15W02	X10	8.70E–01	2029	3300	869	360
44	2003	11/02	17:15	S20W56	X8.3	9.10E–01	2598	1570	476	155
45	2003	11/04	19:29	S19W83	X28.0	2.30E+00	2657	353	59.3	15.3
46	2003	11/20	07:47	N01W08	M9.6	6.00E–02	669	13	0.82	0.26
47	2003	12/2	09:48	S13W65	C7.2	5.10E–03	1393	86	2.28	0.39
48	2004	04/11	04:19	S14W47	C9.6	1.30E–02	1645	35	1.04	0.4
49	2004	07/25	15:14	N08W33	M1.1	6.50E–02	1333	2086	29.1	1.86
50	2004	11/07	16:06	N09W17	X2.0	2.00E–01	1759	495	33.2	4.93
51	2004	11/10	02:13	N09W49	X2.5	1.60E–01	2000	300	49.5	13.2
52	2005	01/15	23:02	N15W05	X2.6	6.30E–01	2861	300	1.93	0.83
53	2005	01/17	09:52	N15W25	X3.8	8.40E–01	2547	400	1330	387
54	2005	01/20	07:01	N14W61	X7.1	1.30E+00	3242	1680	1550	1150

Table 1 — *Continued.*

No. (1)	Year yyyy (2)	Date mm/dd (3)	Time hh:mm (4)	Location (5)	$I_{\rm SXR}$ (SXR peak flux) (6)	$\Phi_{\rm SXR}/10^3$ (erg cm^{-2}) (7)	$V_{\rm CME}$ (km s^{-1}) (8)	I_{10} (pfu) (9)	I_{30} (pfu) (10)	I_{50} (pfu) (11)
55	2005	07/13	14:49	N10W80	M5.0	2.00E–01	1423	10	1.16	0.32
56	2005	07/14	10:55	N10W89	X1.2	3.90E–01	2115	110	14.2	2.63
57	2005	08/22	17:27	S12W60	M5.6	1.70E–01	2378	330	27.2	4.8
58	2006	12/13	02:40	S06W24	X3.4	5.10E–01	1774	698	372	239
59	2006	12/14	22:15	S05W31	X1.5	1.20E–01	1042	215	42.3	13.5
60	2010	08/14	10:05	N17W52	C4.4	9.90E–03	1205	14	1.69	0.63
61	2011	03/07	20:12	N24W59	M3.7	1.20E–01	2125	50	4.66	0.82
62	2011	06/07	06:41	S21W64	M2.5	4.40E–02	1255	72	24.5	12.8
63	2011	08/04	03:57	N15W49	M9.3	5.40E–02	1315	96	20.2	7.79
64	2011	08/09	08:05	N17W83	X6.9	1.90E–01	1610	26	15.4	8.65
65	2011	11/26	07:10	N08W49	C1.2	5.30E–03	933	80	2.91	0.56
66	2012	01/23	03:59	N28W36	M8.7	2.00E–01	2175	6310	422	73
67	2012	01/27	18:37	N27W71	X1.7	3.20E–01	2508	796	136	43.5
68	2012	03/13	17:41	N18W62	M7.9	2.40E–01	1884	469	71.8	21.2
69	2012	05/17	01:47	N12W89	M5.1	9.90E–02	1582	255	124	78.3
70	2012	07/06	23:08	S18W50	X1.1	4.30E–02	1828	25	5.11	2.06
71	2012	07/12	16:49	S16W09	X1.4	4.60E–01	885	96	3.49	0.96
72	2012	07/17	17:15	S17W75	C9.9	2.10E–01	958	136	14.6	4.67
73	2012	09/27	23:57	N08W41	C3.7	9.40E–03	1035	28	3.24	0.6
74	2013	05/22	13:32	N15W70	M5.0	1.40E–01	1466	1660	125	22.9
75	2013	09/29	23:37	N15W40	C1.3	1.10E–02	1179	182	8.81	1.54
76	2014	01/07	18:32	S15W11	X1.2	2.50E+00	1830	1033	185	42.6
77	2014	02/20	07:55	S15W67	M3.0	6.30E–02	948	22	6.67	3.59
78	2014	04/18	13:03	S16W41	M7.3	1.10E–01	1208	58	5.77	2.44
79	2014	09/10	17:45	N16W06	X1.6	3.80E–01	1425	126	7.89	3.19

derived and are shown in Figure 1 for $E > 10$ MeV protons, Figure 2 for $E > 30$ MeV and Figure 3 for $E > 50$ MeV protons.

We can see from Figure 1 that the CCs between I_{10} and $I_{\rm SXR}$ in the three longitudinal areas W0–W39, W40–W70 and W71–W90 are 0.24±0.17, 0.43±0.15 and 0.26±0.24 respectively. It is obvious that the CC between I_{10} and SXR peak flux is longitudinally dependent. The largest CC is only 0.43±0.15 in the well connected region, suggesting that I_{10} has only a weak correlation with $I_{\rm SXR}$ in the well connected region.

We can see from Figure 2 that the CCs between I_{30} and SXR peak flux in the three longitudinal areas W0–W39, W40–W70 and W71–W90 are 0.43±0.15, 0.71±0.09 and 0.35±0.22 respectively. It is evident that the CC between I_{30} and SXR peak flux is highly longitudinally dependent, and the CC between I_{30} and $I_{\rm SXR}$ reaches its largest value in the well connected region and then declines dramatically in the longitudinal area outside the well connected region.

Figure 3 shows that the CCs between I_{50} and $I_{\rm SXR}$ in the three longitudinal areas W0–W39, W40–W70 and W71–W90 are 0.54±0.13, 0.77±0.07 and 0.36±0.22 respectively. The CC between I_{50} and $I_{\rm SXR}$ is highly longitudinally dependent, and the CC between I_{50} and $I_{\rm SXR}$ reaches its largest value in the well connected region and then declines dramatically in the longitudinal area outside the well connected region.

3.2 Correlation between SEPs and SXR Fluence

To check whether the CCs between SXR fluence and the peak flux of SEP events are longitudinally dependent, and compare the CC between SXR fluence and peak intensities of SEP events with the one between SXR peak flux and peak intensities of SEP events, the CCs between SXR fluence and peak intensities of SEP events have been derived and are shown in Figure 4 for $E > 10$ MeV, Figure 5 for $E > 30$ MeV and Figure 6 for $E > 50$ MeV protons.

We can see from Figure 4 that the CCs between I_{10} and Φ_x in the three longitudinal areas W0–W39, W40–W70 and W71–W90 are 0.43±0.15, 0.58±0.12 and 0.39±0.22 respectively. Although the correlation be-

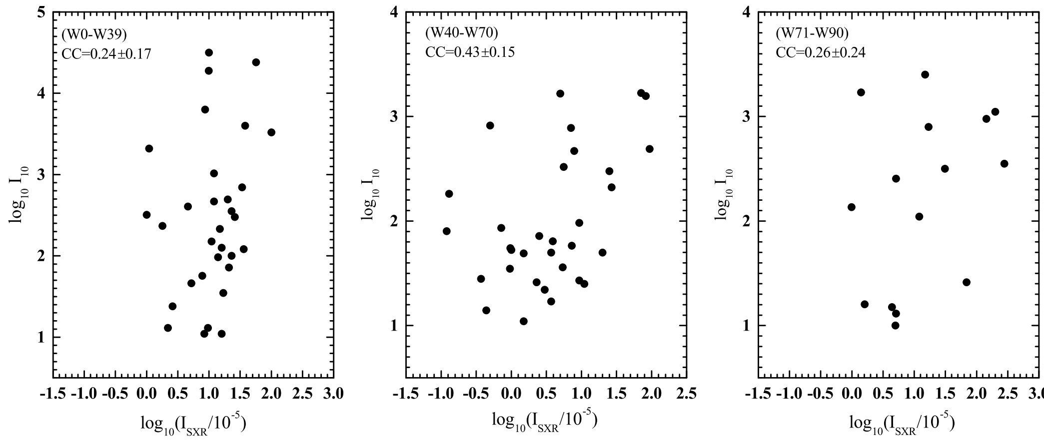

Fig. 1 Scatter (log-log) plots of I_{10} versus $I_{\rm SXR}$ in the three longitudinal areas.

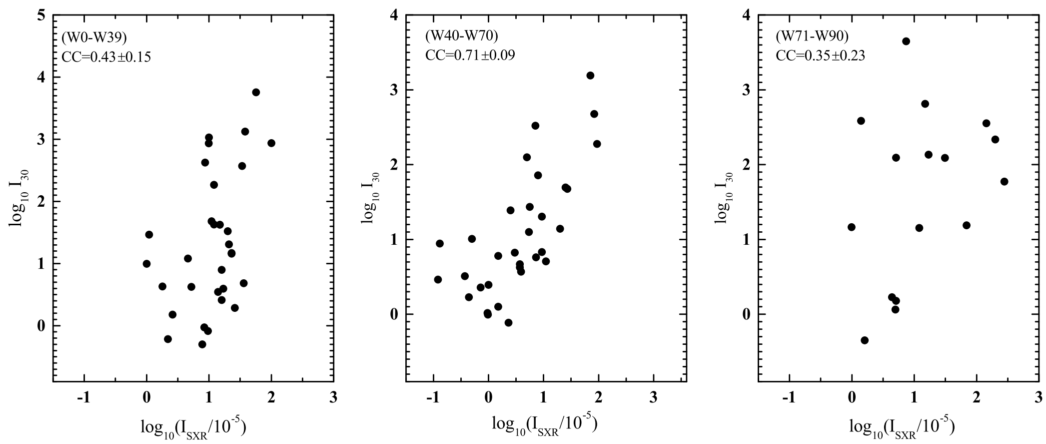

Fig. 2 Scatter (log-log) plots of I_{30} versus $I_{\rm SXR}$ in the three longitudinal areas.

tween Φ_x and I_{10} is moderate in the well connected region, the CC between Φ_x and I_{10} is still highly longitudinally dependent. It evident that Φ_x has a closer association with I_{10} than with $I_{\rm SXR}$.

We can see from Figure 5 that the CCs between I_{30} and Φ_x in three longitudinal areas W0–W39, W40–W70 and W71–W90 are 0.50±0.14, 0.80±0.06 and 0.37±0.22 respectively. It is evident that the CC between I_{30} and Φ_x is highly longitudinally dependent, and I_{30} has a good correlation with Φ_x in the well connected region. The CC between Φ_x and I_{30} is larger than that between $I_{\rm SXR}$ and I_{30} in the well connected region, suggesting that Φ_x has a closer association with I_{30} than $I_{\rm SXR}$. The CC between I_{30} and Φ_x is larger than the one between I_{10} and Φ_x in the well connected region, suggesting that I_{30} has a closer association with Φ_x than I_{10}.

Figure 6 shows that the CCs between I_{50} and Φ_x in the three longitudinal areas W0–W39, W40–W70 and W71–W90 are 0.54±0.13, 0.83±0.06 and 0.13±0.28 respectively. It is evident that the CC between I_{50} and Φ_x is highly longitudinally dependent. The CC between I_{50} and Φ_x is larger than the one between I_{50} and $I_{\rm SXR}$ in the well connected region, suggesting that I_{50} has closer association with Φ_x than $I_{\rm SXR}$. The CC between I_{50} and Φ_x is larger than the one between I_{30} and Φ_x in the well connected region, suggesting that I_{50} has a closer association with Φ_x than I_{30}.

3.3 Correlation between Peak Intensities of SEP Events and CME Speeds

The CCs between the speeds of CMEs and the peak intensities of SEP events with different energies in three longitudinal areas W0–W39, W40–W70 and W71–W90

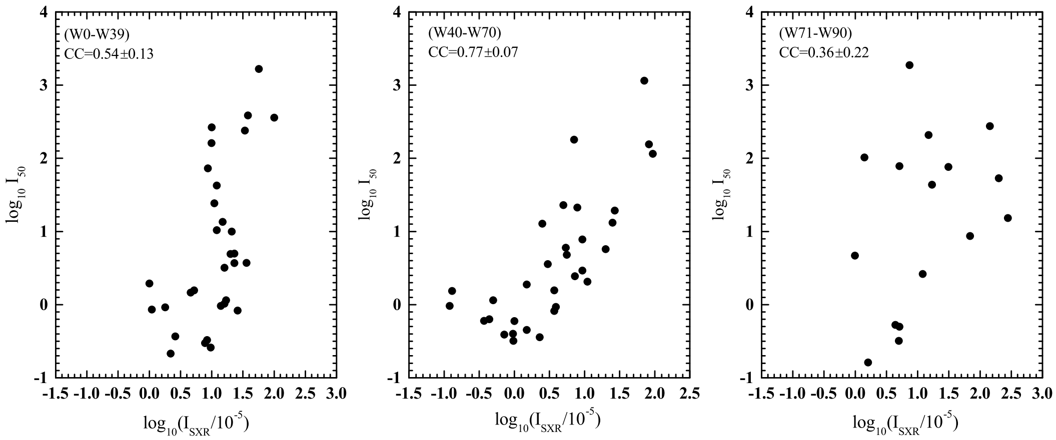

Fig. 3 Scatter (log-log) plots of I_{50} versus $I_{\rm SXR}$ in the three longitudinal areas.

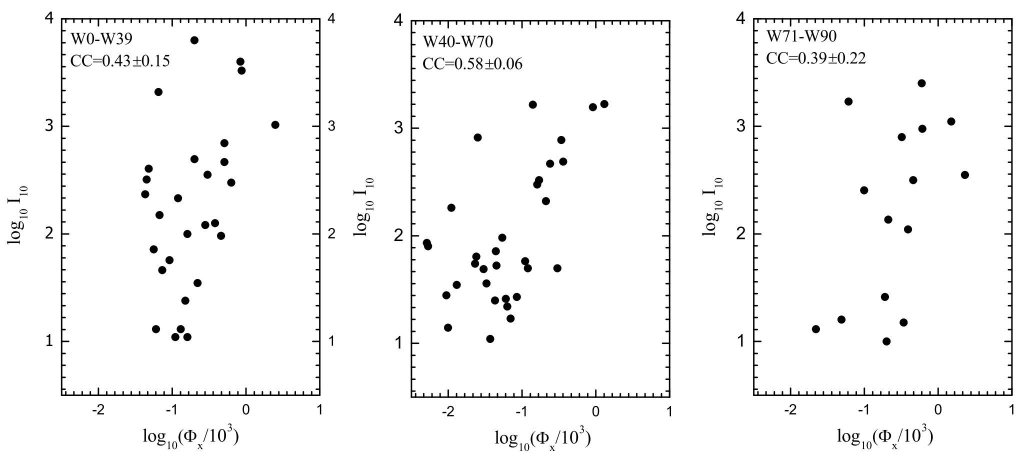

Fig. 4 Scatter (log-log) plots of I_{10} versus Φ_x in the three longitudinal areas.

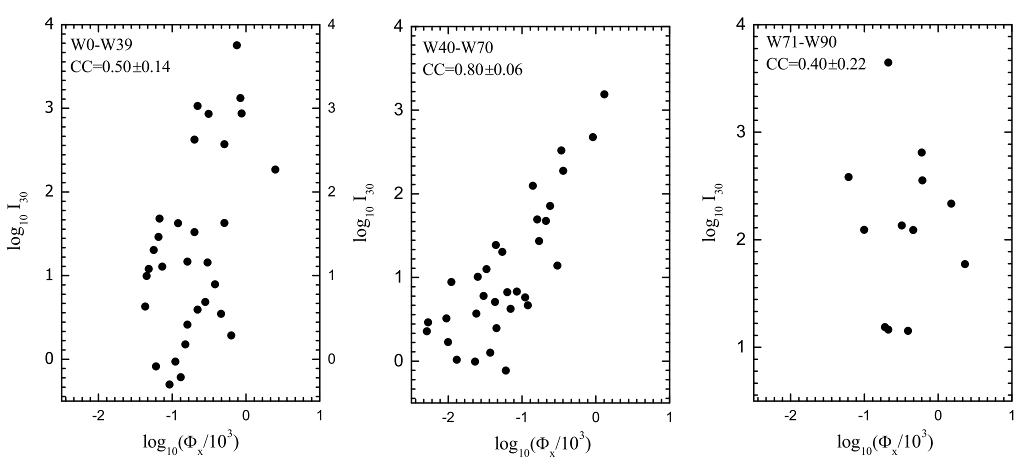

Fig. 5 Scatter (log-log) plots of I_{30} versus Φ_x in the three longitudinal areas.

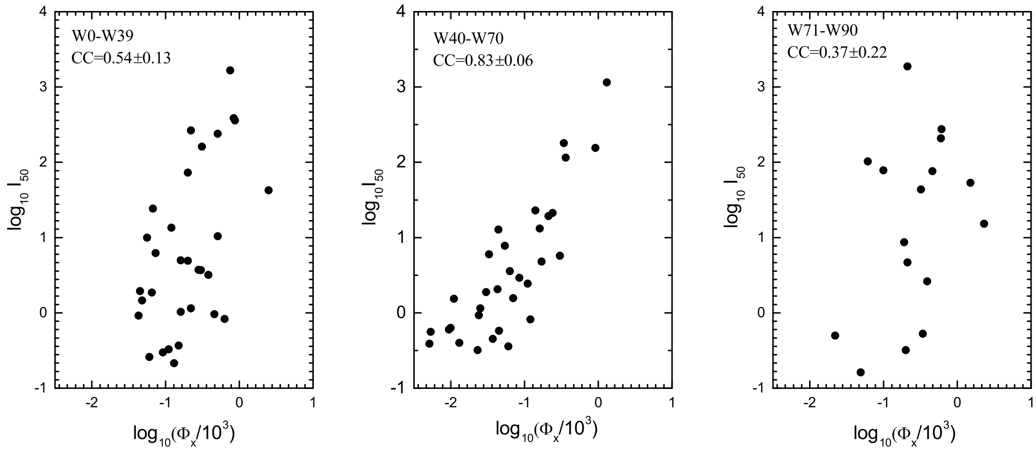

Fig. 6 Scatter (log-log) plots of I_{50} versus Φ_x in the three longitudinal areas.

have been derived and are shown in Figure 7 for $E > 10\,$MeV protons, Figure 8 for $E > 30\,$MeV protons and Figure 9 for $E > 50\,$MeV protons.

We can see from Figure 7 that CCs between I_{10} and $V_{\rm CME}$ in the three longitudinal areas W0–W39, W40–W70 and W71–W90 are 0.67±0.10, 0.56±0.12 and 0.45±0.21 respectively. The CC between $V_{\rm CME}$ and I_{10} is slightly longitudinally dependent and the CC reaches its largest value in the longitudinal area W0–W39.

We can see from Figure 8 that CC between I_{30} and $V_{\rm CME}$ in the three longitudinal areas W0–W39, W40–W70 and W71–W90 are 0.54±0.10, 0.53±0.13 and 0.40±0.21 respectively. The CC in the longitudinal area W0–W39 is almost the same as the CC in the longitudinal area W40–W70.

Figure 9 shows that CCs between I_{50} and $V_{\rm CME}$ in the three longitudinal areas W0–W39, W40–W70 and W71–W90 are 0.50±0.14, 0.48±0.14 and 0.34±0.23 respectively. The difference between the CC in the longitudinal area W0–W39 and the CC in the longitudinal area W40–W70 is only 0.02, which can be ignored.

4 PARTIAL CORRELATION ANALYSIS

Partial correlation between two variables is considered by nullifying the effects of the third (or fourth, or more) variable upon the variables being considered, which has been used by Trottet et al. (2015) to analyze the correlation between peak intensities of 15–40 MeV protons and the parameters of the associated solar activities. To investigate how CME speed, SXR peak flux and SXR fluence independently affect the peak intensities of $E > 10$, $E > 30$ and $E > 50$ MeV protons in the well connected region, the partial CCs between the peak intensities of $E > 10$, $E > 30$ and $E > 50\,$MeV protons and the parameters of associated solar activities, together with statistical uncertainties from the bootstrap method, will be calculated. We use $\mathrm{CC_p}\,(X, Y)$ to indicate the partial CC between parameters X and Y.

4.1 Partial Correlation Analysis for $E > 10\,$MeV Protons

For SEP events with a source location in the well connected region, $\mathrm{CC_p}(\log_{10} I_{10}, \log_{10} V_{\rm CME})$, $\mathrm{CC_p}(\log_{10} I_{10}, \log_{10} I_{\rm SXR})$ and $\mathrm{CC_p}(\log_{10} I_{10}, \log_{10} \Phi_x)$ are 0.46±0.15, -0.36 ± 0.16 and 0.51 ± 0.14 respectively, suggesting that for the SEP events with source location in the well connected region, both CME speed and SXR fluence can significantly affect the peak intensities of $E > 10\,$MeV protons, but SXR peak flux makes no additional contribution.

4.2 Partial Correlation Analysis for $E > 30\,$MeV Protons

For SEP events with source location in the well connected region, $\mathrm{CC_p}(\log_{10} I_{30}, \log_{10} V_{\rm CME})$, $\mathrm{CC_p}(\log_{10} I_{30}, \log_{10} I_{\rm SXR})$ and $\mathrm{CC_p}(\log_{10} I_{30}, \log_{10} \Phi_x)$ are 0.26 ± 0.18, -0.06 ± 0.19 and 0.52 ± 0.14 respectively. It is evident that Φ_x has much better correlation with peak intensity of $E > 30\,$MeV protons than $V_{\rm CME}$, suggesting that for SEP events with source location in the well connected region, only Φ_x can significantly affect the peak intensities of $E > 30\,$MeV protons, while CME shock just makes a small contri-

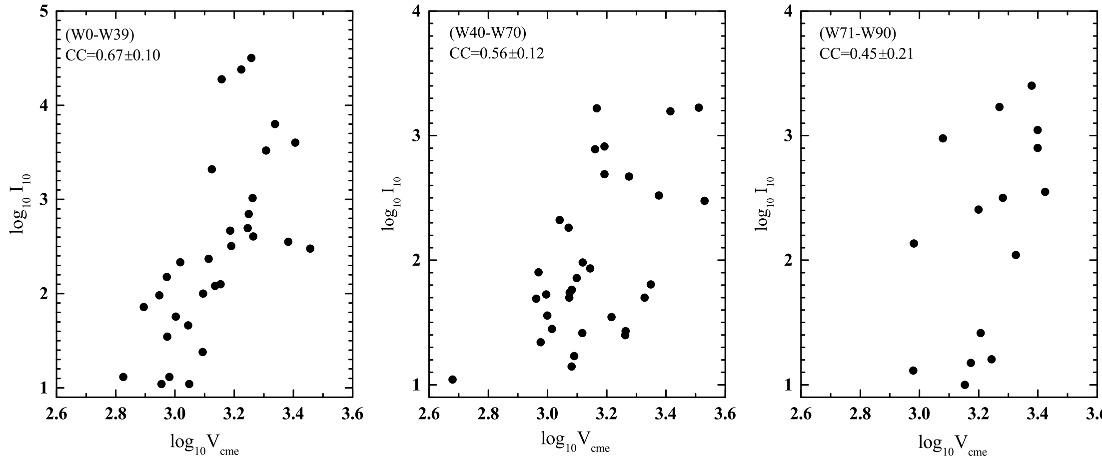

Fig. 7 Scatter (log-log) plots of I_{10} versus $V_{\rm CME}$ in the three longitudinal areas.

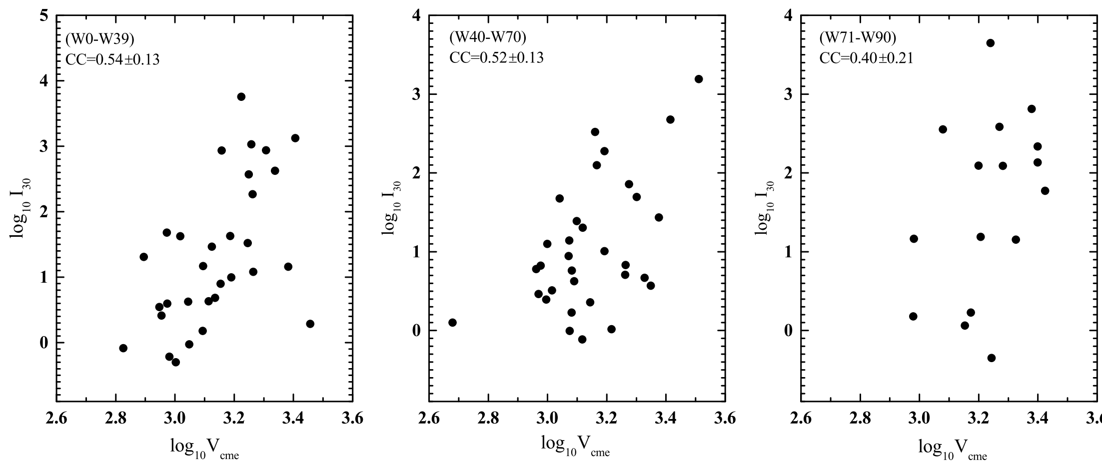

Fig. 8 Scatter (log-log) plots of I_{30} versus $V_{\rm CME}$ in the three longitudinal areas.

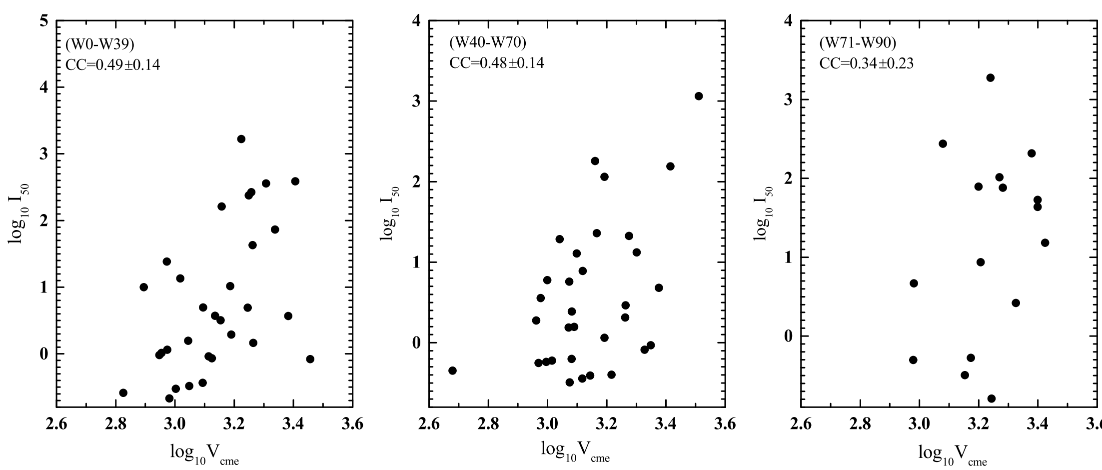

Fig. 9 Scatter (log-log) plots of I_{50} versus $V_{\rm CME}$ in the three longitudinal areas.

bution to the peak intensities of $E > 30\,\mathrm{MeV}$ protons, and I_{SXR} makes no additional contribution the peak intensities of $E > 30\,\mathrm{MeV}$ protons.

4.3 Partial Correlation Analysis for $E > 50\,\mathrm{MeV}$ Protons

For SEP events with source location in the well connected region, $\mathrm{CC_p}(\log_{10} I_{50},\ \log_{10} V_{\mathrm{CME}})$, $\mathrm{CC_p}(\log_{10} I_{50},\ \log_{10} I_{\mathrm{SXR}})$ and $\mathrm{CC_p}(\log_{10} I_{50},\ \log_{10} \Phi_x)$ are 0.11±0.19, 0.11 ± 0.19 and 0.49 ± 0.14 respectively, suggesting that for the SEP events with source location in the well connected region, only SXR fluence can significantly affect the peak intensities of $E > 50\,\mathrm{MeV}$ protons, but both SXR peak flux and CME speed make no additional contribution to the peak intensities of $E > 50\,\mathrm{MeV}$ protons.

5 SUMMARY AND DISCUSSION

If the source locations of SEP events are not well connected with the Earth, the *GOES* spacecraft is located in a poor position to observe the particles accelerated by concurrent flares. However, if the source locations of SEP events are well connected with the Earth, the *GOES* spacecraft is located in a good position to observe flare-accelerated particles. This suggests that if flares really contribute to the production of SEPs in large gradual SEP events, then the CC between flares and the peak intensities of SEP events should be longitudinally dependent, and the CC between flares and SEPs should reach its largest value in the well connected region and decline dramatically in the longitudinal area outside the well connected region. The results of the paper suggest that flares really contribute to production of $E > 10$, $E > 30$ and $E > 50\,\mathrm{MeV}$ protons.

By comparing Figure 1 with Figure 7, we can find that the CC between speeds of CMEs and I_{10} is always larger than the CC between SXR peak flux and I_{10} in the same longitudinal area, suggesting that for $E > 10\,\mathrm{MeV}$ protons, CME speed is more important than flare intensity, which is consistent with the result obtained in the paper Park et al. (2012).

For $E > 10$, $E > 30$ and $E > 50\,\mathrm{MeV}$ protons with source location in the well connected region, classical correlation analyses show that the CC between SXR fluence and peak intensities of SEPs is always larger than that between SXR peak flux and peak intensities of SEPs, suggesting that SXR fluence always has a closer association with the peak intensities of SEP events than SXR peak flux, namely that SXR fluence is a more important parameter describing the relationship between SXR emission and SEP events than SXR peak flux.

For $E > 10\,\mathrm{MeV}$ protons, the combination of classical correlation and partial correlation analyses shows that in the well connected region, both flare and CME shock are effective accelerators for $E > 10\,\mathrm{MeV}$ protons. For $E > 30\,\mathrm{MeV}$ protons, the combination of classical correlation and partial correlation analyses shows that in the well connected region, $E > 30\,\mathrm{MeV}$ protons can be accelerated by both concurrent flares and CME shocks. However, $E > 30\,\mathrm{MeV}$ protons may be mainly accelerated by concurrent flares. For $E > 50\,\mathrm{MeV}$ protons, the combination of classical correlation and partial correlation analyses shows that in the well connected region, $E > 50\,\mathrm{MeV}$ protons may be only accelerated by concurrent flares.

The outstanding property of flare-accelerated particles is that the flux of particles accelerated by flares is highly longitudinal or the CC between flares and the peak intensities of SEP events is highly dependent on heliolongitude. If we do not divide the SEP events into three longitudinal regions shown in the paper, the longitudinal dependence of SEP events on the associated flares cannot be found, which has been proved by Le et al. (2017). It can be noticed that the well connected region may not be exactly in the longitudinal area ranging from W40 to W70. The CCs between flares and peak intensities of SEP should be calculated in many more longitudinal areas to precisely look for the well connected region if the number of samples of large SEP events is large enough.

It can be noticed that the flares, in some cases, are not accompanied by SEP events if the flares are not accompanied by CMEs. Klein et al. (2010) suggested that flare-accelerated particles might be trapped in the flare site if radio emissions at decimeter and longer wavelengths are absent. In other words, the flare is confined. If the solar flare is eruptive, an associated CME can open quite a large amount of magnetic field lines over the AR so that flare-accelerated particles can escape from the AR and then propagate into interplanetary space.

6 CONCLUSIONS

Classical correlation analysis shows that in the well connected region, higher energy protons have a closer association with concurrent flares, while lower energy protons have a better correlation with the speeds of associated CMEs, suggesting that flares are effective accelerators for higher energy protons, while CME shocks are effective accelerators for lower energy protons.

The combination of classical correlation analysis and partial correlation analysis suggests that for SEP events with source location in the well connected region, a CME shock is only an effective accelerator for $E < 30\,\mathrm{MeV}$ protons. However, flares are not only effective accelerators for $E < 30\,\mathrm{MeV}$ protons, but also for $E > 30\,\mathrm{MeV}$ protons, and $E > 30\,\mathrm{MeV}$ protons may be mainly accelerated by concurrent flares.

Statistical results are usually given for the majority of cases. The results of the paper do not rule out the possibility that for SEP events with source locations in a well connected region, a shock driven by an associated CME may play a key role in the production of $E > 30\,\mathrm{MeV}$ protons and even for higher energy protons. The discussion of shock geometry and intensity, and whether this kind of shock is well connected with the Earth, is beyond the scope of this paper.

Acknowledgements We are very grateful to the anonymous referee for her/his reviewing of the paper and for helpful suggestions. This work was jointly funded by the National Basic Research Program of China (973 Program, Grants 2012CB957801 and 2014CB744203), the National Natural Science Foundation of China (Grant Nos. 41074132, 41274193, 41474166, 41304144, 11303017 and 11533005), and the National Standard Research Program (Grant 200710123). The SXR data including the flare start, peak and end times, and the SXR fluence were obtained freely from NOAA (*ftp://ftp.ngdc.noaa.gov/STP/space-weather/solar-data/solar-features/solar-flares/x-rays/goes*). The data on SPEs that occurred during solar cycle 23 were obtained freely from NOAA (*http://spidr.ngdc.noaa.gov/spidr*), while the data on SPEs that occurred during solar cycle 24 were also obtained freely from NOAA (*http://umbra.nascom.nasa.gov/sdb/goes/particle*). The linear speed of each CME is obtained freely from the CME catalog (*http://cdaw.gsfc.nasa.gov/CME_list*).

References

Andriopoulou, M., Mavromichalaki, H., Plainaki, C., Belov, A., & Eroshenko, E. 2011, Sol. Phys., 269, 155
Aschwanden, M. J. 2012, Space Sci. Rev., 171, 3
Aurass, H., Mann, G., Rausche, G., & Warmuth, A. 2006, A&A, 457, 681
Bazilevskaya, G. A. 2009, Advances in Space Research, 43, 530
Bieber, J. W., Matthaeus, W. H., Shalchi, A., & Qin, G. 2004, Geophys. Res. Lett., 31, L10805
Brueckner, G. E., Howard, R. A., Koomen, M. J., et al. 1995, Sol. Phys., 162, 357
Cane, H. V., Richardson, I. G., & von Rosenvinge, T. T. 2007, Space Sci. Rev., 130, 301
Cane, H. V., Richardson, I. G., & von Rosenvinge, T. T. 2010, Journal of Geophysical Research (Space Physics), 115, A08101
Chen, Y., Le, G., Lu, Y., et al. 2016, Ap&SS, 361, 40
Dierckxsens, M., Tziotziou, K., Dalla, S., et al. 2015, Sol. Phys., 290, 841
Firoz, K. A., Gan, W. Q., Moon, Y.-J., & LI, C. 2012, ApJ, 758, 119
Gopalswamy, N., Xie, H., Yashiro, S., & Usoskin, I. 2005, International Cosmic Ray Conference, 1, 169
Grechnev, V. V., Kurt, V. G., Chertok, I. M., et al. 2008, Sol. Phys., 252, 149
Grechnev, V. V., Kiselev, V. I., Meshalkina, N. S., & Chertok, I. M. 2015, Sol. Phys., 290, 2827
Kallenrode, M.-B. 2003, Journal of Physics G Nuclear Physics, 29, 965
Klein, K.-L., Trottet, G., & Klassen, A. 2010, Sol. Phys., 263, 185
Klein, K.-L., Masson, S., Bouratzis, C., et al. 2014, A&A, 572, A4
Kouloumvakos, A., Nindos, A., Valtonen, E., et al. 2015, A&A, 580, A80
Kubo, Y., & Akioka, M. 2004, Space Weather, 2, S01002
Le, G.-M., Tang, Y.-H., & Han, Y.-B. 2006, ChJAA (Chin. J. Astron. Astrophys.), 6, 751
Le, G.-M., Li, P., Yang, H.-G., et al. 2013, RAA (Research in Astronomy and Astrophysics), 13, 1219
Le, G.-M., Li, C., Tang, Y.-H., et al. 2016, RAA (Research in Astronomy and Astrophysics), 16, 14
Le, G.-M., Li, C., & Zhang, X.-F. 2017, RAA (Research in Astronomy and Astrophysics), 17, 073
Li, C., Tang, Y. H., Dai, Y., Fang, C., & Vial, J.-C. 2007a, A&A, 472, 283
Li, C., Tang, Y. H., Dai, Y., Zong, W. G., & Fang, C. 2007b, A&A, 461, 1115
Li, C., Dai, Y., Vial, J.-C., et al. 2009, A&A, 503, 1013
Masson, S., Klein, K.-L., Bütikofer, R., et al. 2009, Sol. Phys., 257, 305
Miroshnichenko, L. I., Klein, K.-L., Trottet, G., et al. 2005, Journal of Geophysical Research (Space Physics), 110, A11S90
Park, J., Moon, Y.-J., Lee, D. H., & Youn, S. 2010, Journal of Geophysical Research (Space Physics), 115, A10105

Park, J., Moon, Y.-J., & Gopalswamy, N. 2012, Journal of Geophysical Research (Space Physics), 117, A08108
Pérez-Peraza, J., Vashenyuk, E. V., Miroshnichenko, L. I., Balabin, Y. V., & Gallegos-Cruz, A. 2009, ApJ, 695, 865
Qin, G. 2007, ApJ, 656, 217
Qin, G., Wang, Y., Zhang, M., & Dalla, S. 2013, ApJ, 766, 74
Qin, G., & Zhang, L.-H. 2014, ApJ, 787, 12
Qin, G., & Wang, Y. 2015, ApJ, 809, 177
Reames, D. V. 1999, Space Sci. Rev., 90, 413
Simnett, G. M. 2006, A&A, 445, 715
Trottet, G., Samwel, S., Klein, K.-L., Dudok de Wit, T., & Miteva, R. 2015, Sol. Phys., 290, 819
Tylka, A. J., Cohen, C. M. S., Dietrich, W. F., et al. 2005, ApJ, 625, 474
Wall, J. V., & Jenkins, C. R. 2012, Practical Statistics for Astronomers (Cambridge: Cambridge Univ. Press)
Yashiro, S., Gopalswamy, N., Michalek, G., et al. 2004, Journal of Geophysical Research (Space Physics), 109, A07105